A SYSTEM FOR REAL AMPLITUDE RECOVERY IN LAND SEISMIC RECORDINGS†

SUDHIR JAIN*

ABSTRACT

A system to recover the real relative amplitude variations in seismic reflection profiles recorded with binary gain data over land has been developed. This compensates for the spherical divergence and the inelastic losses, computes the variations due to shot and receiver locations and the spread geometry, suppresses noise-bursts like frost-breaks and applies corrections based on all these factors. The capacity is provided to estimate first-break times which can be used in computation of weathering corrections. An example of the processing of real data is presented to illustrate different components of the system. This shows that meaningful true amplitude sections can be obtained even when the signal to noise ratio is poor and strong noise trains and extensive near-surface variations are present.

INTRODUCTION

A seismic reflection event conveys useful information about the composition of the subsurface in any or all of the following three modes:

1. Time of arrival.
2. Frequency distribution, which manifests itself as the shape of the wavelet.
3. Amplitude of the reflection.

Traditionally, the first two features of the reflections are preserved and, when possible, enhanced during processing. However, the information conveyed by the amplitude of the reflection is distorted severely during normal recording and processing by the application of A.G.C., equalization and normalization at various stages. In very recent years, the advent of binary gain recording and true amplitude processing has reduced the excessive use of A.G.C. and equalization during processing. Indeed, in ideal circumstances where all shots inject identical amounts of energy into the subsurface, all receivers are planted uniformly and losses in the low-velocity layer are uniform, desired information on lateral variation of amplitudes for a particular reflection can be obtained merely by avoiding arbitrary scaling, by correcting the recorded amplitudes for spherical divergence and inelastic losses (Dobrin 1950) at some stage of processing and by recording and displaying the data with fixed gain.

Unfortunately, the actual situation is far from ideal, particularly in on-shore recordings. The effective strength of the source varies irregularly, geophones are impossible to plant with any uniformity, the low velocity layer has variable transmission characteristics, unpredictable noise-bursts occur on records and most often the traces display energy distribution which is related to the distance from the source even when

†Paper presented at the 44th Annual International SEG Meeting, Dallas, Texas, November 11-14, 1974, and the Joint C.S.E.G.-C.S.P.G. Convention in Calgary, May 1975. Manuscript received by the Editor June 8, 1975; revised manuscript received September 29, 1975.

*Digitech Ltd., Calgary, Alberta, Canada.

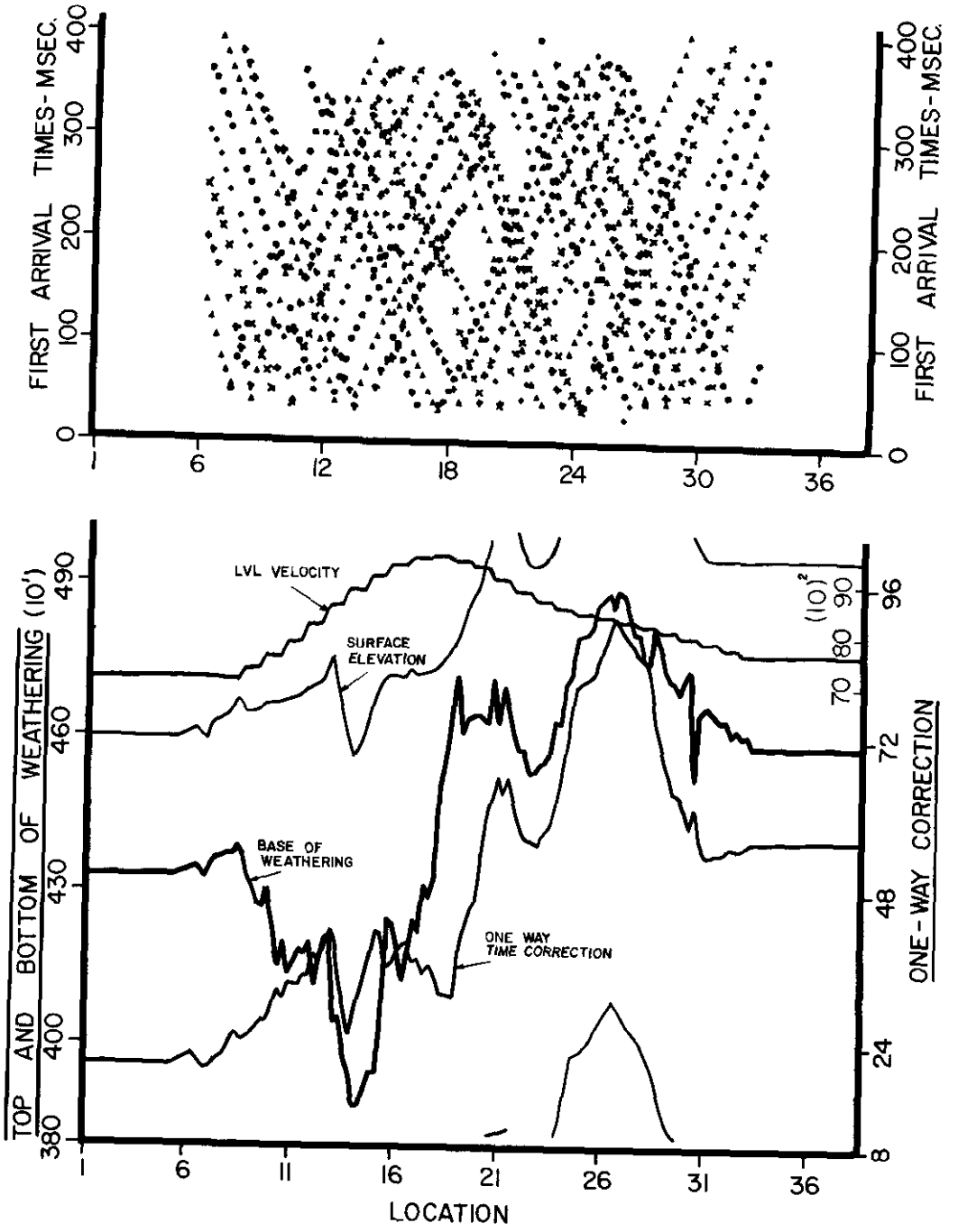
FIRST ARRIVAL TIMES-MSEC.
0
100
200
300
400
1
6
12
18
24
30
36
LVL VELOCITY
SURFACE ELEVATION
BASE OF WEATHERING
ONE WAY TIME CORRECTION
TOP AND BOTTOM OF WEATHERING (10')
380
400
430
460
490
(10)²
70
80
90
96
ONE-WAY CORRECTION
8
24
48
72
1
6
11
16
21
26
31
36
LOCATION

Fig. 1.

spherical divergence has been applied. To analyze the amplitudes of reflections in these circumstances, all these factors have to be properly compensated during the processing of the data. A record of these corrections must be available if the final interpretation is to indicate the existence of amplitude anomalies of further interest.

This paper describes a technique for statistically determining the amplitude corrections required to be adequately applied to the recorded data.

Types of Amplitude Variations

The amplitude variations on a seismic section which are of interest in interpretation of data can be divided into four categories.

1. Vertical or travel-time dependent variations.

2. Lateral variations due to one or more of the following:

(a) Subsurface geology.

(b) Effective coupling to the ground of source and receiver patterns.

(c) Transmission losses due to differences in low velocity layer at both source and receiver ends.

(d) Energy received at different distances from the source. This factor is perhaps related to spread geometry and source and receiver patterns.

3. Sudden noise-bursts like frost-breaks or cultural noise which can be severe enough to distort the amplitudes in the stacked sections even if only occasional field traces suffer from these disturbances.

4. Bad shots and/or seismometer groups which may cause either dead or very energetic isolated traces. These energetic traces usually do not contain much valid information.

Description of Truamp

A program called TRUAMP was written for a UNIVAC 1106 computer. The program computes the amplitude corrections for factors listed above and applies these corrections to recorded traces. The corrections are plotted on a flatbed plotter on the same scale as the final section so that a direct comparison is available to the interpreter. Another program, AMP, picks specified reflections on processed sections and plots the amplitudes of these events in absolute numbers and in decibels.

Input Requirements:

The input to TRUAMP is binary gain recorded data corrected for the recorded gain. The program needs no information about the data other than spread geometry and the data itself. The velocity distribution, if available, may be submitted. Facility is provided to edit specified traces while reading data, although the program determines wild and weak traces. These traces are omitted in the computation of the amplitude correction factors and may be optionally edited while applying corrections.

Program Functions:

The program reads input traces and does the following:

(1) The onset times of first-break arrivals are determined. The algorithm, similar to one described by Sims and Mackenzie (1973), is also used to determine if traces are wild or too weak to contain valid information. The invalid traces are omitted from subsequent calculations. The refraction times may be used to compute the weathering statics manually or automatically. The plot from one such automatic process is shown in Figure 1.

(2) If present, the noise-bursts which are not related to genuine seismic reflection energy are identified. The energy of these noise-bursts is reduced to the general level of the trace so that the trace may be used in subsequent processing.

(3) The trace is divided into small adjacent segments of specified length and the energy level is computed over each of these. These computations are used to estimate travel-time dependent variations. Spherical divergence corrections are applied based either on travel-time alone or on both velocity and travel-time. Then a second degree polynomial is fitted to the new

energy levels so that inelastic losses may be estimated. The addition of a t^2 term to the inelastic loss equation is intended to compensate for errors in velocity function if they exist. Actual experience showed that this term is of some importance in obtaining appropriate compensation for energy losses. Figure 2 shows an example of the plot of time-dependent variations.

B. The RMS values for the traces are now arranged in the order of common receiver locations (Figure 4).

C. And in the order of common source locations (Figure 5).

The lines showing high frequency variations in both plots are actual variations

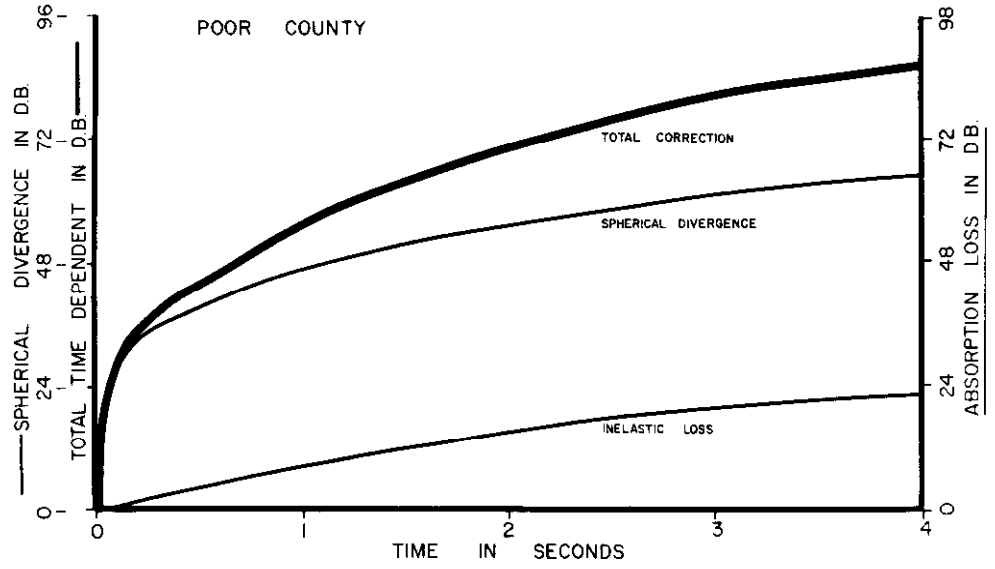

Fig. 2.

(4) Average energy level for a trace is obtained after correcting for the time-dependent losses. These energy levels are grouped together in the following three arrangements:

A. In the order of distance from the source, a least mean square second degree polynomial is computed for the values of energy levels associated with traces in each record. A correction which may be called the "distance from the source correction" is then computed and applied to energy levels computed thus far before the subsequent steps are initiated (Figure 3). Note that this correction is computed after spherical divergence and inelastic losses have been applied. In our experience, the further traces may show energy losses of up to 6 Db or more as compared to nearby traces. This loss is probably due to different responses of the receiver patterns to the wave-fronts approaching them at different angles.

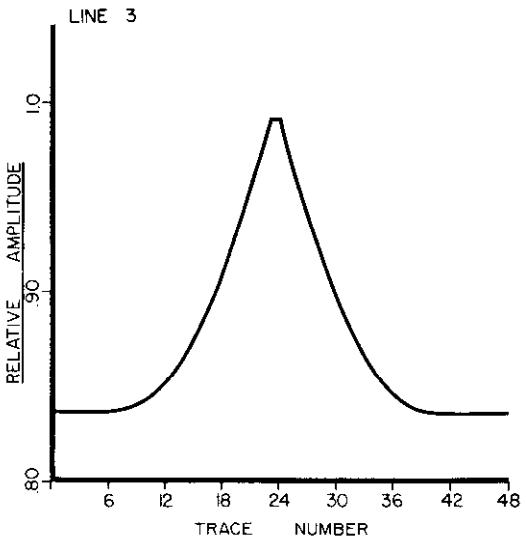

Fig. 3.

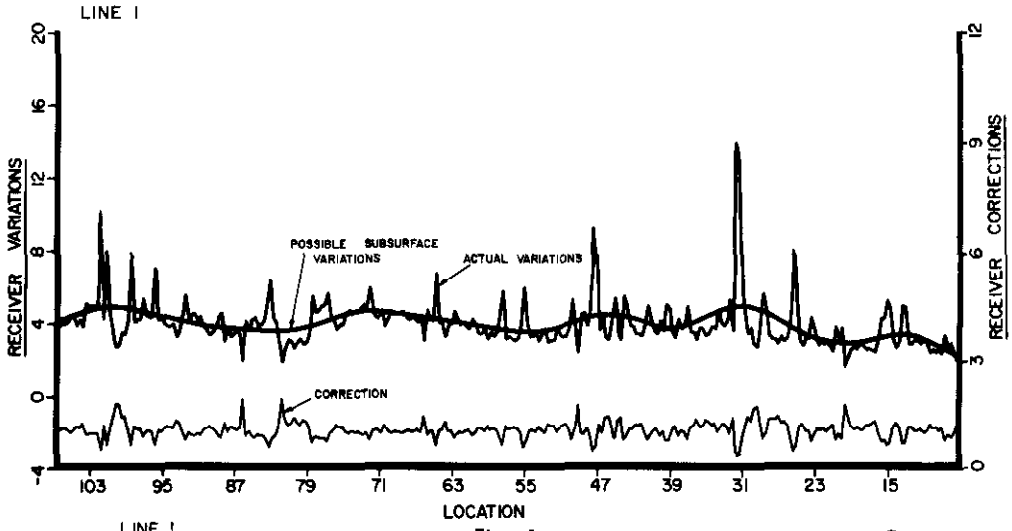

Fig. 4.

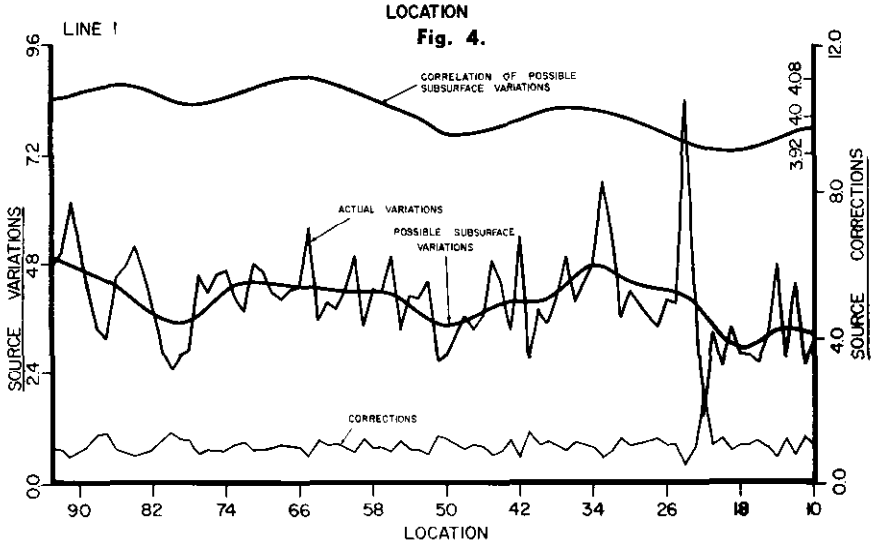

Fig. 5.

associated with the receiver locations (Figure 4) and the source locations (Figure 5). The scale for these variations is given on the left hand side. As expected the actual amplitudes show considerable fluctuations. High frequency components of these variations are due to near-surface causes, associated with the weathering or the shot and geophone coupling. Gradual low frequency variation shown in both plots may be due to subsurface causes which we want to explore or indeed due to gradual variations in the near-surface. Since it is not possible to separate the low frequency variations into near-surface or subsurface components, the corrections are computed for high frequency variations only. These are shown by the lowest curve, with the scale for these at the right.

The fourth curve on the top of Figure 5 shows the 'correlation' of the low frequency variations in the two plots. The 'correlation' is actually the zero lag cross-correlation over the distance of one spread length across each point in both curves. This curve brings out the similarity in the source and receiver variations. If the low frequency curves are similar for a particular variation, this is quite likely to be due to

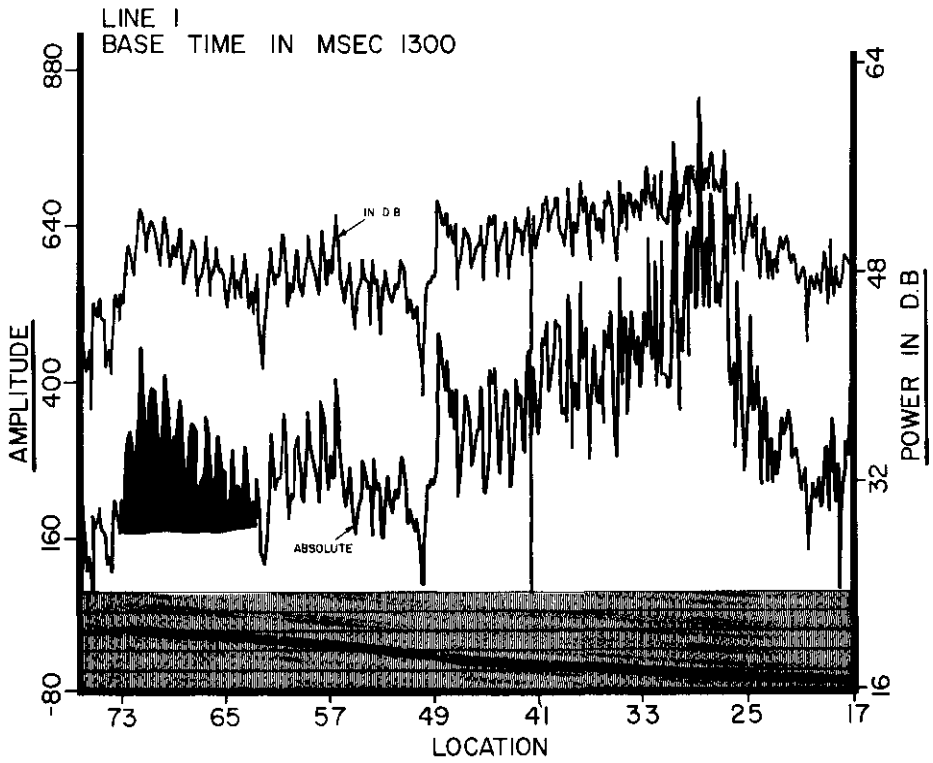

Fig. 6.

near surface. In the example being shown, most of the variations appear to be due to the near-surface.

For purposes of the corrections associated with source and receiver locations, the frequencies with wave-lengths less than the spread length are assumed to be associated with the near-surface. The frequencies with wave-lengths greater than the spread lengths are ascribed to possible (though not definite) subsurface variations.

When the corrections have been computed for a segment of the line, these are applied to the input data and corrected traces are written out on a new tape.

5. To display the amplitude of the stacked data, a plot shown in Figure 6 is generated. This plot is termed Reflection Amplitude Plot and it has three curves. The specified reflections are automatically traced and shown by the bottom curve. The maximum (or minimum) amplitudes corresponding to the reflection on each trace are plotted in absolute values and in decibels. The absolute scale is shown to the left and decibel scale to the right.

Application on Real Data

The example line is taken from the Arctic Islands. Forty-eight traces per shot were recorded with the shot placed between groups 8 and 9, offset by two group intervals from both groups. The group interval was 165 feet. The data was shot for 8-fold stack. The original processing was done with moderate AGC and the stacked section showed very good signal to noise ratio and continuous events down to four seconds.

Figure 7 is the TRUAMP section after stack. Figure 8 shows the section after standard processing with moderate A.G.C. The continuity of the reflections is perhaps slightly better in the section with A.G.C. However, in terms of character of reflections and their correlation across faults, the TRUAMP section offers many advan-

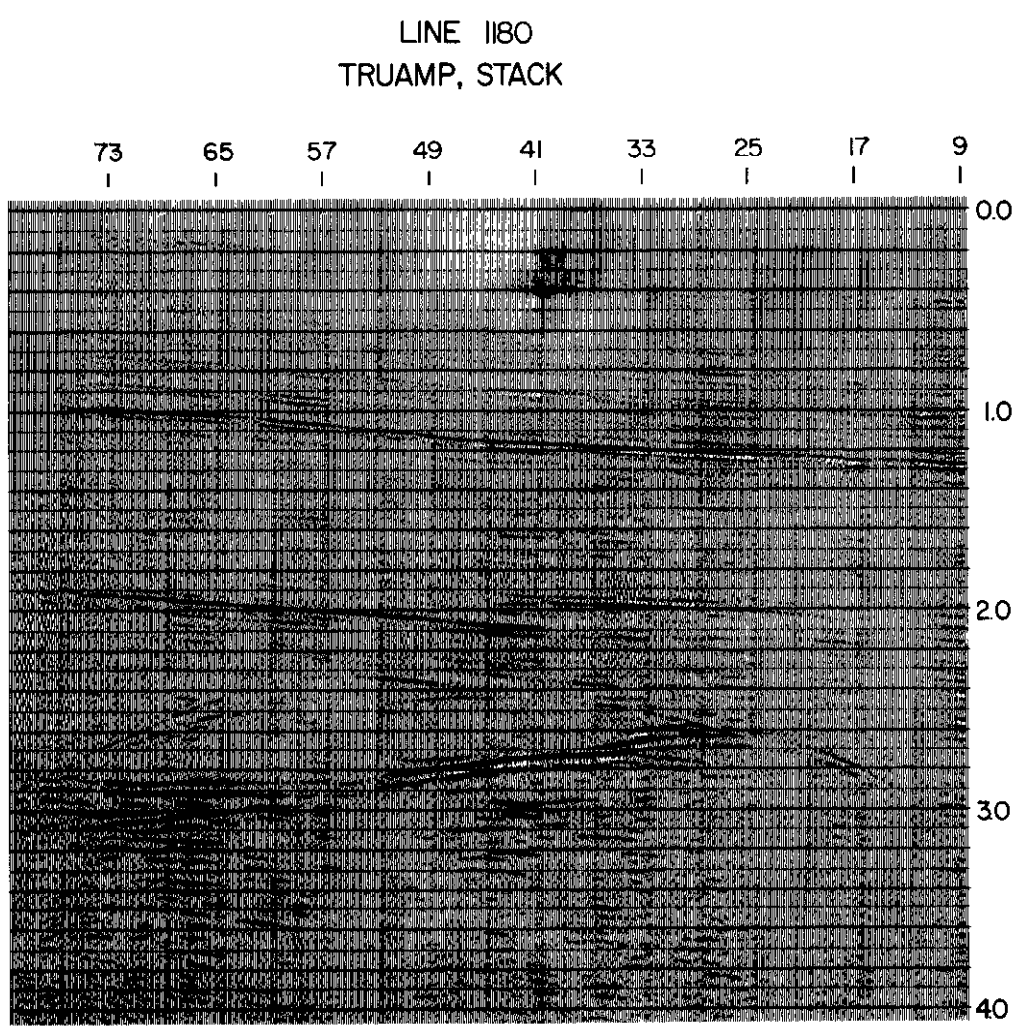

Fig. 7.

tages. One extra advantage not visible on the section, is the fact that digital migration can be achieved more successfully on a true amplitude section. A migrated version of Figure 7 is shown in Figure 9. Note the successful collapse of diffractions between 2.5 and 3.0 seconds at each end. Also note the clarification of the interpretation of the deepest event.

In both stack and migrated sections, the strong reflection which dips from about 1.0 secs. in the west to 1.3 secs. to the east, shows two zones of strong amplitudes, one centered at station 34 and the other between 65 and 75. The reflection amplitude plot (Figure 6) pinpoints these anomalies. To find their source, we look at the receiver plot (Figure 4) and source plot (Figure 5), both of which show that the general amplitude levels are higher where the eastern anomaly is located while in the region of the western anomaly, amplitude levels are lower. The reflection amplitude plot for the deeper event at 2.1 secs. (Figure 10) shows the amplitude increase in the east, but not in the west.

All these plots suggest that of the two amplitude anomalies, only the western one is genuine and the one to the east is quite possibly due to better transmission charac-

teristics in the near surface layer(s). As it turns out, the western anomaly is associated with sands bearing hydrocarbon. It is doubtful that the eastern anomaly will ever be tested.

Conclusion

During the true amplitude processing of on-shore seismic reflection recordings it is essential that the corrections are made for lateral variations introduced by weathering, shot and receiver geometry, array patterns and various other factors. The example illustrated here (and many others) shows that the effects of many of these factors can be separately identified and corrected. Thus, a meaningful true amplitude section can be obtained which offers more valid information than either AGC processed data or the conventional true amplitude processing. Several auxiliary plots generated during these computations provide valuable information to the interpreter and are important interpretation aids in their own right.

Acknowledgements

The author acknowledges the invaluable assistance of Mladen Grahalic who did most of the processing described here.

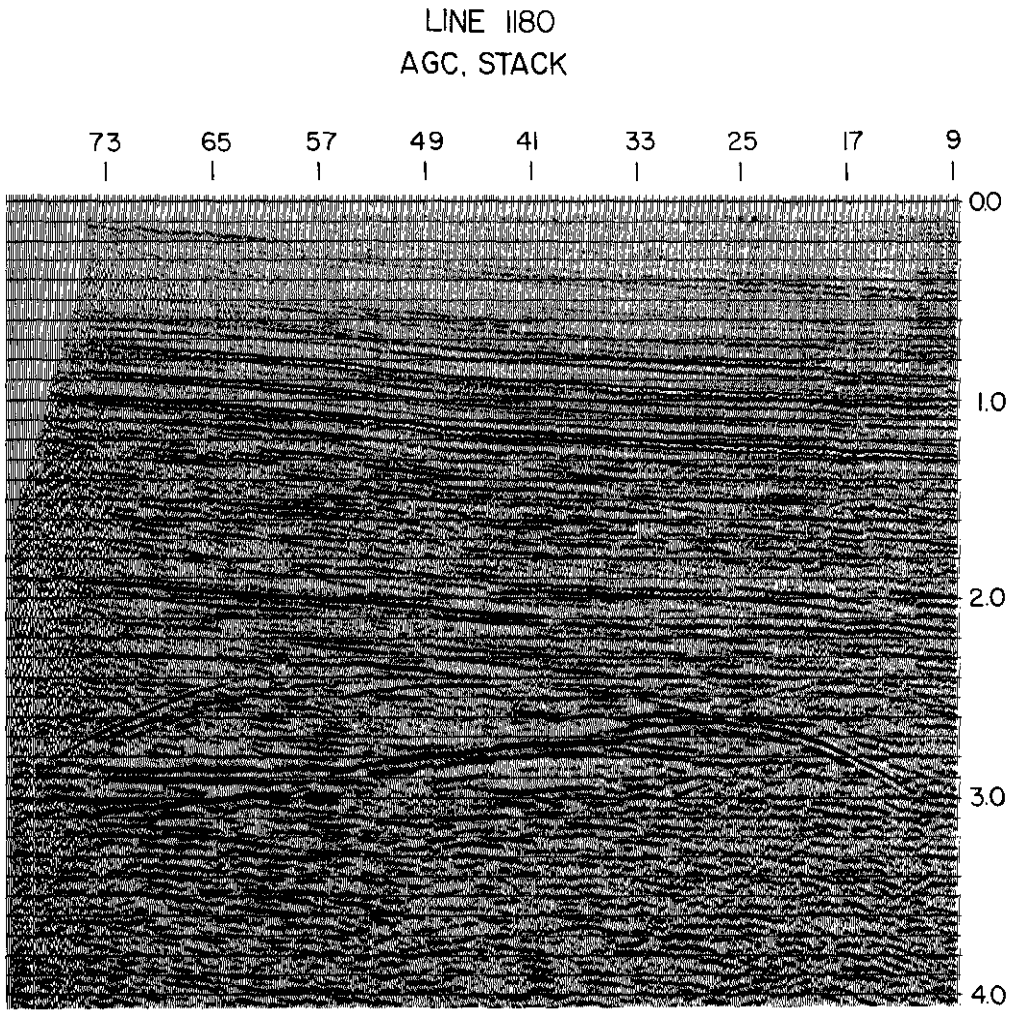

Fig. 8.

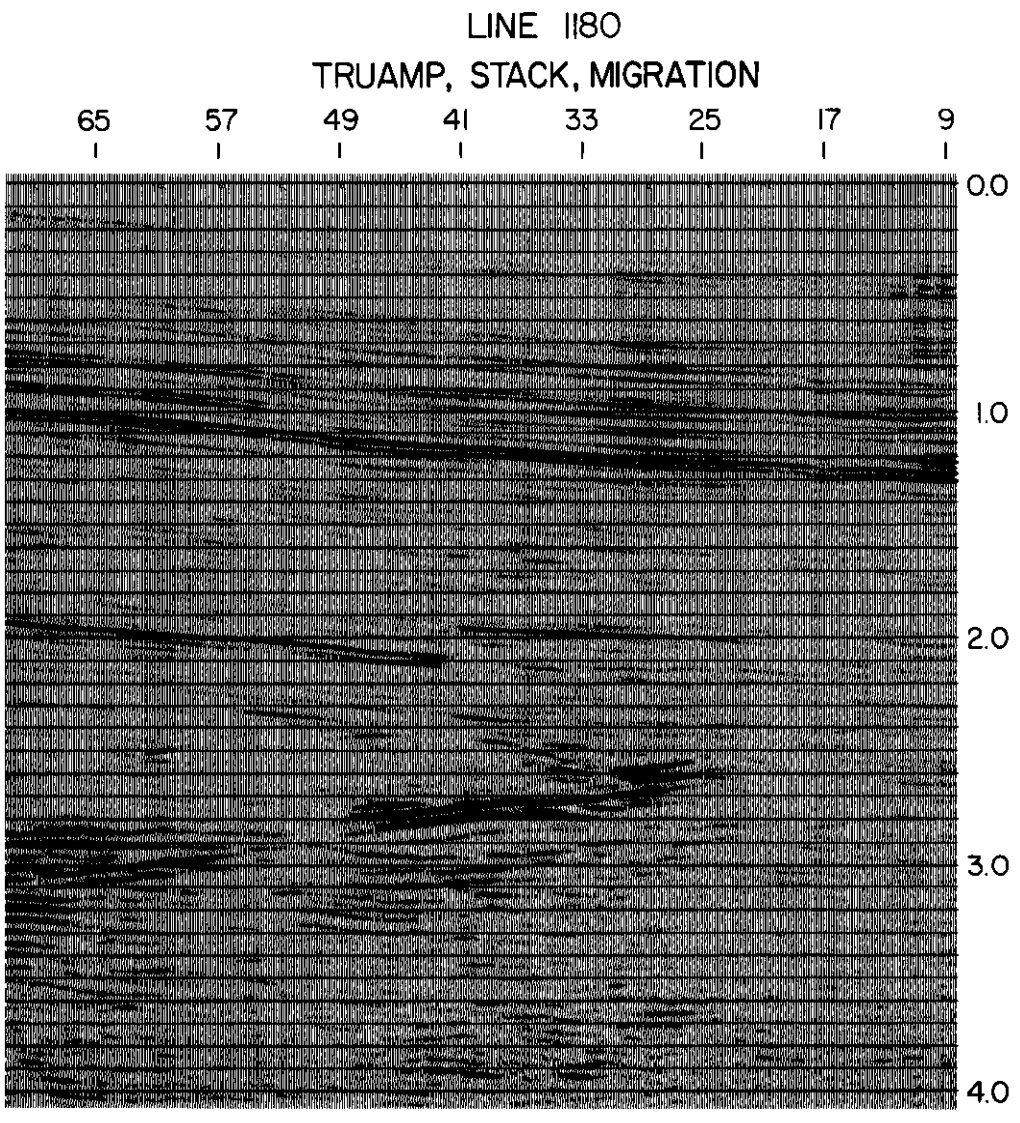

Fig. 9.

Murray Wolfe offered several interesting suggestions during the development of the system. Don Simpson read the draft and suggested improvements. Cheryl Kempster (preparation of manuscript) and Dan Elms (graphics) contributed during the preparation of the paper.

Unfortunately, the oil companies who made the data available for this presentation cannot be revealed without giving away the forbidden information about data. Needless to say, without their kindness this presentation would not have been possible.

References

Dobrin, M. B., 1950, Introduction to Geophysical Prospecting, McGraw Hill, New York.

Sims, J. and Mackenzie, B. E., 1973, 'Computer P-Wave Picking', The Oil & Gas Journal, February 19, 1973.

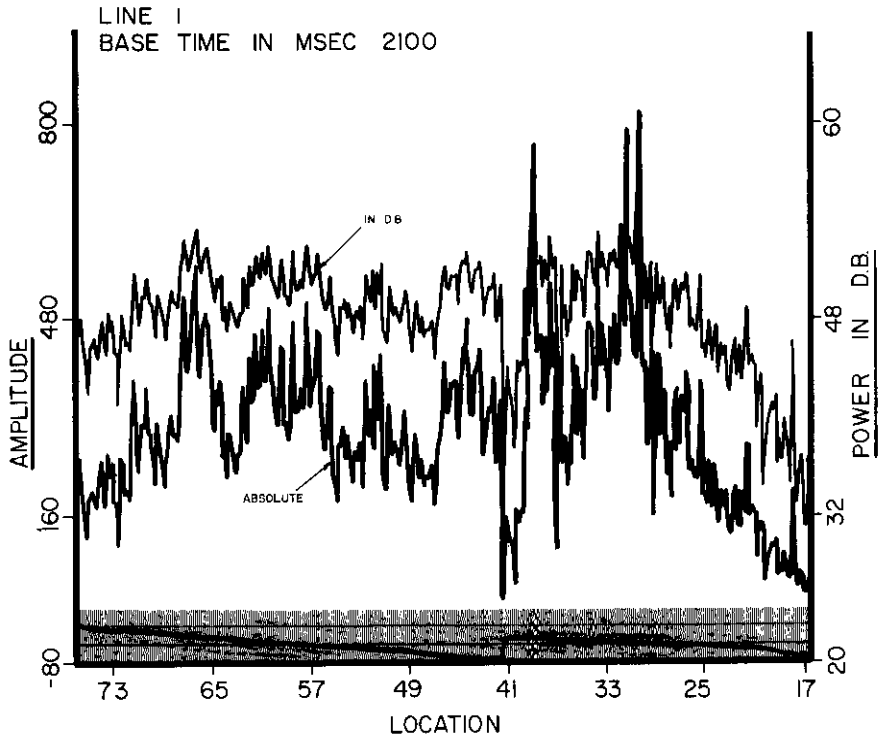
LINE I
BASE TIME IN MSEC 2100
800
480
160
-80
AMPLITUDE
IN DB
ABSOLUTE
60
48
32
20
POWER IN D.B.
73
65
57
49
41
33
25
17
LOCATION

Fig. 10.